

## Optimized Near Minimum Time Control of Flexible Structures Using Variable Gain (LQG) Control Strategies

**Rajiv Kumar**

Lecturer

Dept. of Industrial Engg.,

National Institute of Technology,

Jalandhar-144011, Punjab, India

e-mail: rajivsharma1972@yahoo.com

**S. P. Singh**

Associate Professor

Dept. of Mech. Engg.,

Indian Institute of Technology,

New Delhi-11016, India

e-mail: singhsp@mech.iitd.ernet.in

**H. N. Chandrawat**

Dean (R&SP) & Professor (Retd.)

Dept. of Mech. Engg.,

Thapar Institute of Engineering and Technology,

Patiala-147001, Punjab, India

*A neural network based time optimal control of flexible structures is presented. The implementation is done on a flexible inverted L structure with surface-bonded piezoceramic sensors/actuators. The state-space presentation, from control input voltages to sensor output voltages is established in multivariable form. A variable gain multi-input multi-output linear quadratic regulator controller is designed and implemented. The controller gains are varied as the modal energy of the system decreases. The gains are varied in such a manner that the system utilizes maximum control energy from fixed amplitude of control voltage. The gains are calculated by solving the Riccati equation with weightage in performance index that varies according to the states of the system. Thus at periodic intervals, the gains are updated to fully utilize the available control voltage. Comparison of the present technique is done with the classical bang-bang controller.*

[DOI: 10.1115/1.2166856]

Contributed by the Technical Committee on Vibration and Sound of ASME for publication in the JOURNAL OF VIBRATION AND ACOUSTICS. Manuscript received June 30, 2004; final manuscript received August 30, 2005. Assoc. Editor: Shirley J. Dyke.

### 1 Introduction

With the development of new materials, a trend of using piezoelectric materials as distributed actuators/sensors has emerged. A large body of research work is available using piezoelectric materials for vibration control. Bailey and Hubbard [1], proposed Constant Amplitude and Constant Gain Control algorithms. Crawley and de Luis [2] analyzed the stiffness effect of piezoelectric actuators on the elastic properties of the host structure. Baz and Poh [3] studied the vibration of smart structures by modified independent modal space control by taking the effect of bonding layer between piezoceramics actuators and the host structure. Tzou et al. [4] investigated the piezoelectric effect on the vibration control through a modal shape analysis.

In the case of flexible structures, it is desirable that the vibrations once induced, should die out as quickly as possible. This concept is called minimum time control. Distributed control of a flexible, thin walled tube in pure torsion using Lyapunov control law has been demonstrated theoretically as well as experimentally by Spearritt and Ashokanathan [5]. An energy formulation was introduced in this study which enabled prediction of optimum actuator configuration. The Lyapunov controller used in this study can provide maximum energy extraction, hence minimum time control for given amplitude of control voltage. The main problem in this technique was that the PVDF film actuators can easily be destroyed due to abrupt change of control voltage. The life of the PZT actuators also decreases due to this problem. Ashokanathan et al. [6] solved this problem up to some extent by using modified Lyapunov control law. In this method the constant voltage supplied to the actuators was replaced by continuous-time voltage.

In the present study, multivariable linear quadratic regulator (LQR) is used with time varying gains. As the modal energy of the system decreases, the value of the gains is changed in such a way that the maximum control energy can be utilized by the system via actuators, for reducing the vibration amplitude. Gains are calculated off-line and are classified into various classes based on the states of the system using learning vector quantization (LVQ) neural networks. As the states of the system are lowered (i.e., vibration amplitude is lowered), gains are identified in real time using trained neural networks. Since all the gains are calculated offline using the Riccati equation, the control effort required for the system to send from any initial condition to zero state is optimal in performance index sense. At the same time, the updating of gains at periodic intervals helps in better utilization of control effort available, thus further reducing the settling time.

### 2 Mathematical Modeling of Smart Structures

In the present study, an inverted L structure as shown in Fig. 1 is considered for analysis. The structure is mounted with two piezoceramic patches on its surface acting as actuators and other two piezoceramic patches bonded on surface acting as sensors. Lagrange's equations of motion for linear systems are

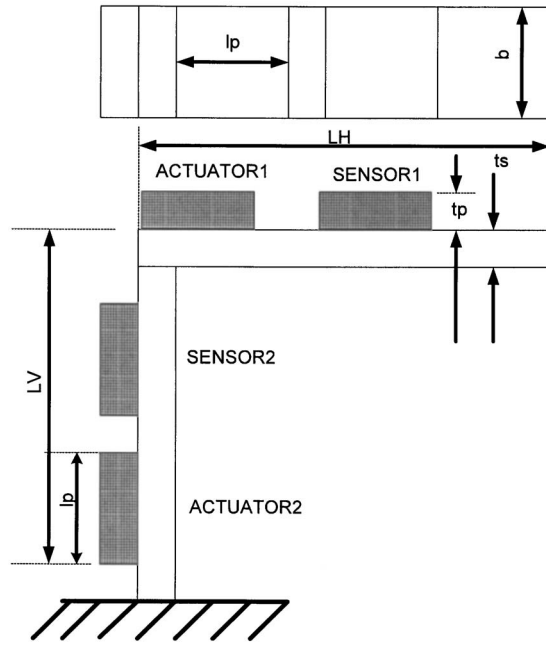


Fig. 1 Inverted L structure

$$\sum_{s=1}^n [m_{js}\ddot{y}_s(t) + c_{js}\dot{y}_s(t) + k_{js}y_s(t)] = Q_j(t), \quad j = 1, 2, \dots, n \quad (1)$$

where  $y_s(t)$  is the physical displacement,  $\dot{y}_s(t)$  is physical velocity, and  $\ddot{y}_s(t)$  is the acceleration at time instant  $t$  for the  $s$ th degree of freedom. In addition  $m$ ,  $c$ , and  $k$  are the elements of mass, damping, and stiffness matrices, respectively. Relation (1) represents a set of  $n$  simultaneous second-order ordinary differential equations in generalized coordinates. By this relation, the infinitely many-degree-of-freedom distributed system is approximated by an  $n$ -degree of freedom system. This relation can be written in matrix form as

$$\mathbf{M}\ddot{\mathbf{y}}(t) + \mathbf{C}\dot{\mathbf{y}}(t) + \mathbf{K}\mathbf{y}(t) = \mathbf{Q}(t) \quad (2)$$

where  $\mathbf{M}$ ,  $\mathbf{C}$ , and  $\mathbf{K}$  are the global mass, damping, and stiffness matrices, respectively, and  $\mathbf{Q}(t)$  is the vector of physical applied forces at various degrees of freedom on an instant of time  $t$ . The column vector  $\mathbf{y}(t)$  represents the nodal displacements at time  $t$ . Using these global mass and stiffness matrices, the frequencies and mode shapes of the system can be obtained. When a piezoelectric patch, attached to the distributed structure, is subjected to a change in slope at its two edges, electric charge is developed inside the system. This charge developed in the PZT patch mounted on a steel structure is given as (Buttler and Rao [7])

$$\delta(t) = \frac{1}{2}(t_s + t_p)(d_{31} + \nu_p d_{32}) \frac{E_p}{1 - \nu_p^2} b [\theta_2(t) - \theta_1(t)] \quad (3)$$

where  $\theta_2(t)$  and  $\theta_1(t)$  are, respectively, the slopes of end 1 and end 2 of the PZT patch at the instant of time  $t$ . The thickness of steel and PZT patch are denoted by  $t_s$  and  $t_p$ , respectively. The dielectric constants of the PZT material are denoted by  $d_{31}$  and  $d_{32}$ . The breadth of the steel beam and piezoelectric patch is denoted by  $b$ . The value of Young's modulus of elasticity and Poisson's ratio for the PZT material are denoted by  $E_p$  and  $\nu_p$ , respectively. Similarly the value of Young's modulus of elasticity and Poisson's ratio for the steel beam are denoted by  $E_s$  and  $\nu_s$ , respectively. The values of these parameters are given in Tables 1 and 2. The voltage developed due to this charge is

Table 1 The geometrical and mechanical properties of the inverted L structure

Material Property	STEEL	PZT
Length of horizontal limb (mm)	$L_H = 100$	
Length of vertical limb (mm)	$L_V = 100$	
Thickness (mm)	$t_s = 1$	$t_p = 1$
Length (mm)	$l_s = 20$	$l_p = 20$
Width (mm)	$B = 10$	$b = 10$
Young's modulus (MPa)	$E_s = 210$	$E_p = 64$
Density (Kg/m <sup>3</sup> )	$\rho_s = 7800$	$\rho_p = 7650$

$$V(t) = \frac{\delta(t)t_p}{\epsilon_p A_p} \quad (4)$$

where  $A_p$  is the area of PZT patch, and  $\epsilon_p$  is the permittivity of the PZT material. Since all values except  $\theta_1(t)$  and  $\theta_2(t)$  are constant in Eqs. (3) and (4), Eq. (4) may be written as  $V(t) = \Gamma[\theta_2(t) - \theta_1(t)]$ , where  $\Gamma$  is a conversion coefficient. On the other hand, when a voltage  $V$  is applied across the piezoelectric patch, the bending moment  $M_f$  of opposite sense is produced at both the edges. The value of this bending moment is given as (Baz [3])

$$M_f = \left[ \frac{d_{31} b E_p (E_s t_p t_s + E_s t_b^2)}{2(E_p t_p + E_s t_s)} \right] V \quad (5)$$

Since all the parameters except  $V$  are constant in relation (5), it may be written as  $M_f [\text{N m}] = \Psi V [\text{V}]$ , where  $\Psi$  is the conversion coefficient and its units are  $\text{N m V}^{-1}$ . To construct the system model from control input to sensor output voltages, relations (4) and (5) are used. For a system having  $r$  modes, the system dynamics can be written in matrix state space form as given below:

$$\dot{\mathcal{W}}(t) = \mathcal{F}\mathcal{W}(t) + \mathcal{G}u(t) \quad (6)$$

$$y(t) = \mathcal{H}\mathcal{W}(t)$$

where the modal state vector is defined as

$$\mathcal{W}(t) = \begin{bmatrix} w_1 & (t) \\ w_2 & (t) \\ w_3 & (t) \\ w_4 & (t) \\ \vdots & \\ w_{2r-1} & (t) \\ w_{2r} & (t) \end{bmatrix}$$

such that  $\mathcal{F}$ ,  $\mathcal{G}$ , and  $\mathcal{H}$  are system matrices and can be obtained from matrices  $\mathbf{M}$ ,  $\mathbf{K}$ , and  $\mathbf{C}$ , Meirovitch [8,9]. Digitizing the continuous-time system into discrete-time system, following system is obtained in terms of system matrices  $\mathbf{A}$ ,  $\mathbf{B}$ , and  $\mathbf{C}$

$$\begin{aligned} \mathbf{X}(k+1) &= \mathbf{A}\mathbf{X}(k) + \mathbf{B}u(k) \\ \mathbf{y}(k) &= \mathbf{C}\mathbf{X}(k) \end{aligned} \quad (7)$$

Using the gain matrix  $\mathbf{K}$ , control inputs are calculated as

Table 2 The electrical properties of the inverted L structure

Property	Symbol	Value
Piezoelectric charge constant ( $\text{m V}^{-1}$ )	$d_{31}$	$1.71 \times 10^{-10}$
Piezoelectric charge constant ( $\text{m V}^{-1}$ )	$d_{32}$	$1.71 \times 10^{-10}$
Poisson's ratio	$\nu_p$	0.28
Permittivity ( $\text{F m}^{-1}$ )	$\epsilon$	$1.06 \times 10^{-10}$

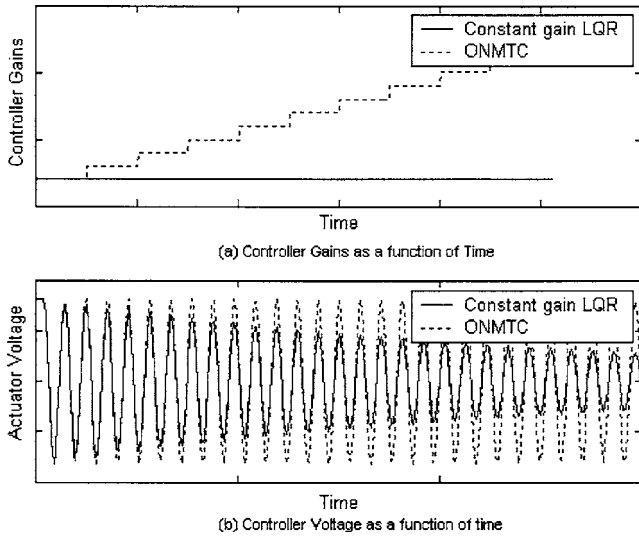


Fig. 2 Concept of optimized near minimum time control

$$\mathbf{u}(k) = -\mathbf{K}\mathbf{X}(k) \quad (8)$$

The gain matrix  $\mathbf{K}$  is evaluated using the system matrices and the weighing matrices  $\mathbf{Q}$  and  $\mathbf{R}$ .

### 3 Concept of Optimized Near Minimum Time Control

An objective of the present control strategies is to obtain the minimum setting time with peak voltage as a constraint. As the states of the system change, modal energy of the system also changes. The input voltage applied to actuators is a function of the states of the system. In LQR, the system utilizes less control voltage at lower modal energies. By updating the control gains as modal energy changes, it is possible to utilize the actuator voltage in a better way. This results in lesser settling time for the disturbed system. Since, in constant gain LQR, the controller gains are designed by considering the highest states (i.e., states corresponding to highest vibration amplitudes) of the system, controlling the system at lower states (i.e., states corresponding to lower vibration amplitudes) utilizes lower voltages, hence non-optimal use of available peak voltage. In constant gain LQR, the control gains are calculated once and these gains remain fixed for the entire control process. However, better use of available control voltage can be made by recalculating the control gains during the process based on relative weightage of matrices  $\mathbf{Q}$  and  $\mathbf{R}$ . The recalculation can be done intermittently in order to reduce the computational complexity of the system.

**3.1 Gains Classification Based on States of the System.** As stated above, the problem of supplying much lower actuator voltages at lower states may be avoided by modifying the control gains. It is, however, not practical to use control gains varying continuously as a function of time. It is, therefore, suggested that the control gains may be varied intermittently as shown in Fig. 2(a). This figure shows that as the modal energy decreases (i.e., vibration amplitude decreases); next higher value of gains should be applied. This would enable the controller to apply nearly the available peak voltage to actuators even at lower states, i.e., lower amplitudes (Fig. 2(b)). The values of control gains at each time step are obtained by re-solving the Riccati equation. These gains are calculated off-line and depend on the modal energy. Since modal energy calculations at each time step is not computationally efficient, the gains selection based directly on states is more appropriate as compared to classification based on modal energy. The computational speed is not decreased since complex calculations to find modal energies are avoided. Because every class belongs to the same system and its gains calculated from Riccati

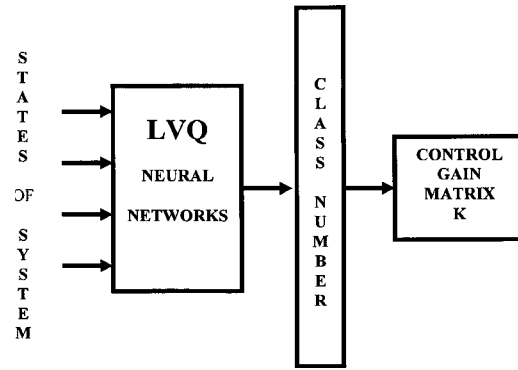


Fig. 3 Implementation of LVQ for gains classification

equation satisfy the stability criterion, the system is inherently stable. At the most there will be sub-optimal use of the available peak voltage for that period of time if a different class is identified. Considering these factors the system classification based on the states of the system is chosen. Two different approaches were tried in the present study for gain selection. The approximation technique by using Back propagation neural networks was used to find the mapping between system states and the control signals.

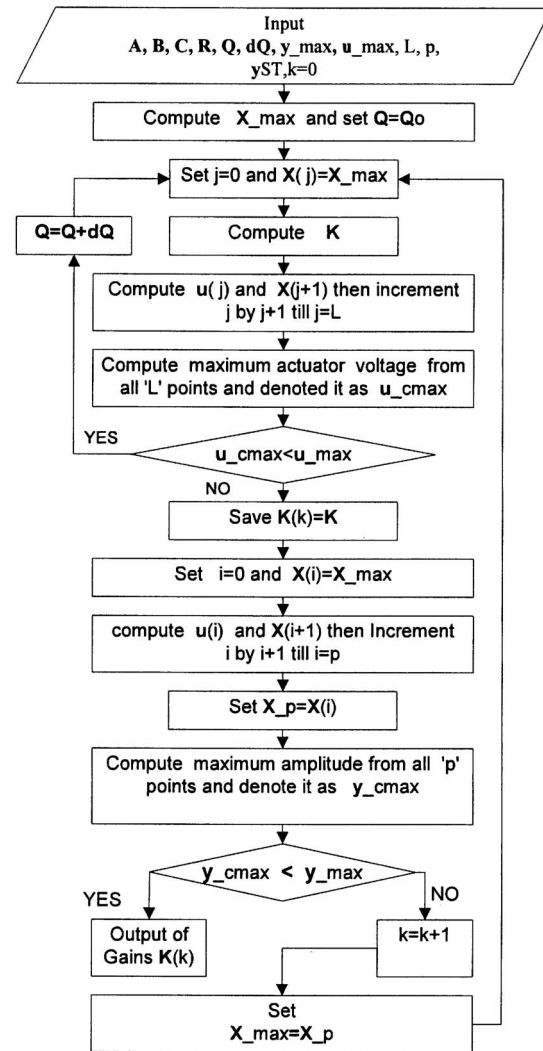


Fig. 4 Algorithm for computation of sets of gains for optimized near minimum time control

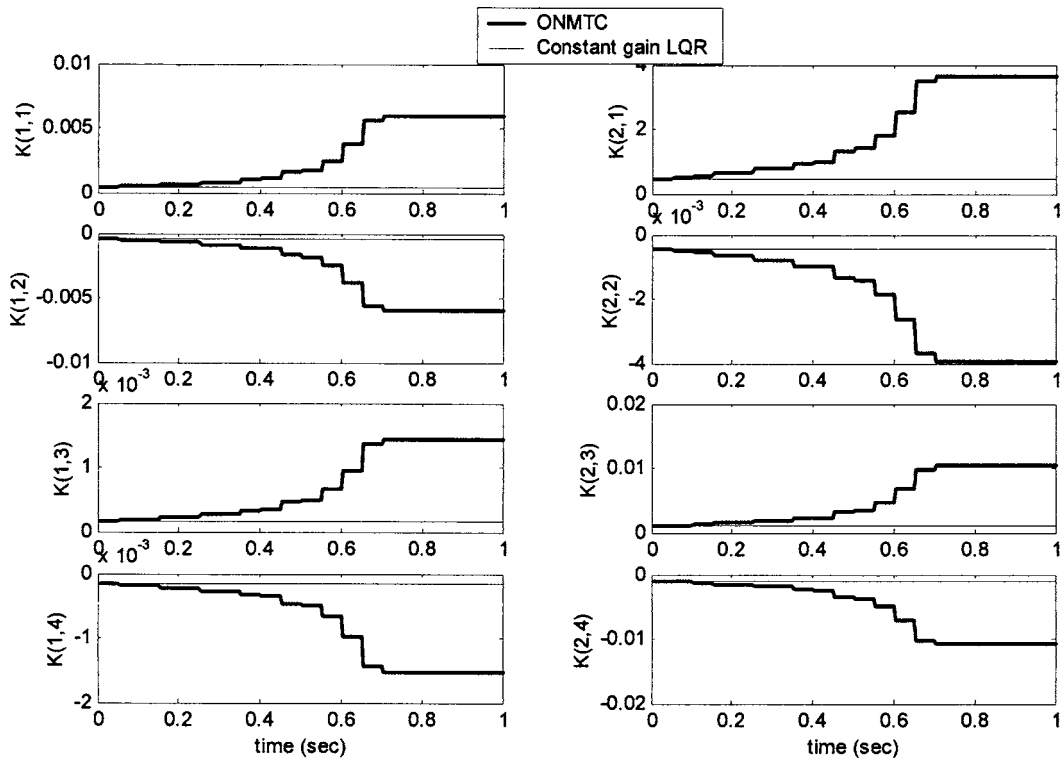


Fig. 5 Time varying controller gains

However, this approach sometimes leads to divergent results due to two reasons: Neural networks approximate continuous function up to any desired accuracy. However, functions, which are not always continuous, are difficult to be mapped. Second, the exact states are not calculated, but only the observer estimated states are used.  $\mathbf{K}(k)$  is the gain matrix and  $\mathbf{X}(k)$  is the state vector at time step  $k$ . Since the gain matrix remains constant at various intervals of time, it is difficult to map this type of function using neural networks.

The second approach, i.e., system classification technique as shown in Fig. 3 is found to always give stable results. Because sometimes, even if the different class is identified, at the most there will be sub-optimal use of the available control voltage for a small interval of time. The states are not being directly used in control signal calculations, i.e., first the gain matrix is identified based on the states of the system, afterwards it is used to calculate the control vector based on the system states.

### 3.2 Optimized Near Minimum Time Control (ONMTC)

**Algorithm.** Figure 4 shows the flow chart of the algorithm for finding out the set of gains that are used to implement ONMTC. The computation is done off-line and set of gains are stored as a function of states. For implementing ONMTC, the gain matrix is retrieved from these stored values for the specified states using trained neural network discussed later. The algorithm works as discussed below.

System matrices  $\mathbf{A}$ ,  $\mathbf{B}$ , and  $\mathbf{C}$  are given as input. Weighing matrices  $\mathbf{R}$ ,  $\mathbf{Q}$ , and the incremental matrix  $d\mathbf{Q}$  are defined. Permissible value of maximum physical deflection is specified and corresponding to this value, the maximum voltage developed at the sensors is found. The vector  $\mathbf{y}_{\max}$  is defined with its elements equal to the maximum voltage developed at sensors. Peak available voltage for the actuators,  $\mathbf{u}_{\max}$  is also defined. In the present implementation, the peak voltage was assumed to be equal to 150 V. The initial settling time  $T$  for open loop response is determined as the time required by the system to reach a sensor

voltage of  $\mathbf{y}_{\text{ST}}$  (i.e., settling amplitude) starting from  $\mathbf{y}_{\max}$ . The value of  $\mathcal{L}$  (i.e., the number of time steps for reaching up to settling amplitude) is calculated using the following relation  $\mathcal{L} = T/t$ , where  $t$  is the sampling interval. However, it is not necessary to calculate the response at all the  $\mathcal{L}$  points. Here we introduce another parameter  $L$  that represents the maximum number of time steps used to completely observe the behavior of the closed-loop system starting from any given state vector. During this transient portion, it is not certain that the maximum applied voltage at the actuators will occur at the start with initial state vector as  $\mathbf{X}_{\max}$ . The maximum value of control voltage can occur at any time step from 0 to  $L$ . For the case study used in this paper, the transient response was needed only up to  $L=30\%$  of  $\mathcal{L}$ . The value of  $L$  was chosen as 300 in the present work to observe the transient behavior.

The parameter  $p$  represents the time steps during which a particular gain matrix is kept constant. These time steps should be carefully selected. Too small time steps increase the number of gains and cause problems in gain classification. Too large time steps, on the other hand, do not give smooth operation of the controller, as the actuator voltage does not remain nearly constant

Table 3 The comparisons of various parameters based on different control strategies

Parameter Method	Settlingtime (Second)	Control effort ( $\text{N m}^2 \text{ s}) \times 10^{-5}$	Input voltage range(V)
Open-loop	2.6		
Constant gain	1.2	2.30	150
LQG			
ONMTC	0.6	4.58	150
EHVC	0.6	11.92	493.14
Bang-band	0.58	13.73	150
Control			

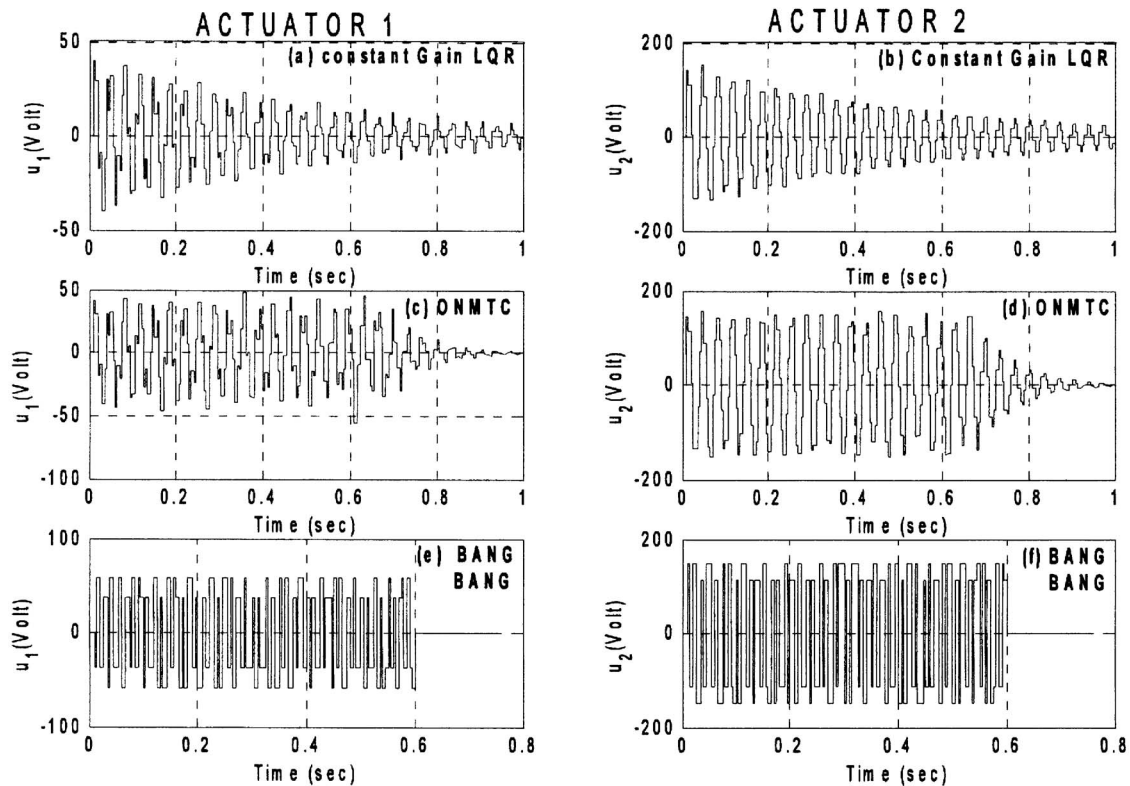


Fig. 6 Voltage applied at actuators for various control strategies

during the entire time span. In the present work  $p$  is taken as 10, which means gains are updated after 10 times the sampling period.

When the system is switched on (Fig. 4), state vector  $\mathbf{X}_{\max}$  is computed using the given value of output vector  $\mathbf{y}_{\max}$ . Then the gain matrix  $\mathbf{K}$  is computed which is to be used during next  $p$  time steps. Next value of gain matrix is calculated using  $\mathbf{X}_{\max}$  computed after  $p$  time steps. The computation of gains continued till the system settles to the desired level.

In this manner, the gain matrix  $\mathbf{K}$  corresponding to each state vector is calculated. Since in  $\mathcal{L}$  steps, gain matrix is to remain constant during every  $p$  steps, thus the total number of  $\mathcal{L}/p$  classes of gain matrices are made. However, the total number of classes used are less than this, because the vibration amplitude reduces earlier in a closed-loop system.

**3.3 Learning Vector Quantization Neural Networks for ONMTC.** For real implementation of the ONMTC, the proper selection of gain matrices at various system states is necessary. Neural network based “learning vector quantization” technique is used for this type of supervised classification (Zurada [10]). Total numbers of “gain matrices” are classified based on the “system states” (Fig. 3). All the states starting from the initial states to end states, and the corresponding control gain matrices are tabulated. Neural network is trained for this tabulation. After each 10 sampling points, the trained LVQ neural network is simulated to obtain the new class of the gain matrices. The gain matrix is retrieved from the memory for that particular class number. Since in simulating the trained neural network, only few additions and multiplications are required, the computational burden is very less, thus, making the real time implementation of the ONMTC easier.

#### 4 Implementation on L Structure

For implementing the optimized near minimum time control theory, inverted L structure is considered. Figure 5 shows the

variation of various elements of the gain matrix as a function of time. It is also obvious from the figure that all the elements of the gain matrix are changing with time as opposed to that used in constant gain LQR. The closed loop damping ratios for different modes of the system depend upon the gain matrix. The damping ratios of both the modes continue to increase with the passage of time as controller gains are increased. The increasing damping ratios reduce the overall settling time of the system. Table 3 gives a comparative picture of settling time and peak voltage requirements obtained from various control methods. To obtain the same effect as by ONMTC, higher control voltages must be applied using constant gain LQR. This type of control is named as “Equivalent High Voltage Control” (EHVC) for reference. By using the input signals at various actuators, the control effort can be obtained from the following relation

$$\text{Control effort} = \sum_{k=0}^{\text{Settling time}} [u_1^2(k)t + u_2^2(k)t] \quad (9)$$

where  $t$  is the sampling time,  $u_1(k)$  and  $u_2(k)$  are the control signals at the actuators at time instant  $k$ . In case of ONMTC, the actuator voltage remains at higher values, in contrast to constant gain LQR, in which actuator voltages are decreased as the system states are lowered. This comparison is shown in Fig. 6. This figure shows that the control forces at both the actuators remain near the available control voltage.

#### 5 Conclusions

As the modal energy of the total system decreases, the gains of the system are updated such that the damping provided to the system increases. In constant gain LQR, the system’s “controller gains” remain constant. Due to this, damping provided to the system remains constant. While with varying gains in Optimized Near Minimum Time Control method, system is imparted higher damping at lower amplitudes (i.e., modal energies). This reduces the overall settling time of the system. Using this new control

method, controller effectiveness can be increased with limited amplitude of control voltage. Since all the gain matrices are calculated using the Riccati equation, the resulted control method is optimal. The gain matrices corresponding to the various system states are classified. And the classes are recalled using neural network based algorithm, thus saving the computational burden of resolving the Riccati equation during every update.

## References

- [1] Bailey, T., and Hubbard, J. E., 1985, "Distributed Piezoelectric—Polymer Active Vibration Control of a Cantilever Beam," *J. Guid. Control Dyn.*, **8**(5), pp. 605–611.
- [2] Crawley, E. F., and de Luis, J., 1987, "Use of Piezoelectric Actuators as Elements of Intelligent Structures," *AIAA J.*, **25**(10), pp. 1373–1385.
- [3] Baz, A., and Poh, S., 1988, "Performance of Active Control System With Piezoelectric Actuators," *J. Sound Vib.*, **126**(2), pp. 327–343.
- [4] Tzou, H. S., 1991, "Distributed Modal Identification and Vibration Control of Continua: Theory and Applications," *ASME J. Dyn. Syst., Meas., Control*, **113**, pp. 494–499.
- [5] Spearritt, D. J., and Ashokanathan, S. F., 1996, "Torsional Vibration Control of a Flexible Using Laminated PVDF Actuators," *J. Sound Vib.*, **193**(5), pp. 941–956.
- [6] Ashokanathan, S. F., and Gu, M., 1997, "Modified Lyapunov Control Law for Torsional Vibration Suppression Using Laminated PVDF Actuators," *Proceedings of the American Control Conference*, Albuquerque, New Mexico, pp. 3552–3556.
- [7] Buttler, R., and Rao, V., 1996, "A State-Space Modeling and Control Method for Multivariable Smart Structural Systems," *Smart Mater. Struct.*, **5**, pp. 386–399.
- [8] Meirovitch, L., 1986, *Elements of Vibration Analysis*, McGraw Hill Publishing Company, New York.
- [9] Meirovitch, L., 1986, *Dynamics and Control of Structures*, John Wiley and Sons, New Delhi.
- [10] Zurada, J. M., 1994, *Introduction to Artificial Neural Systems*, Jaico Publishing House, Mumbai, India.